2005 American Control Conference
June 8-10, 2005. Portland, OR, USA

An Adaptive Neural Network Controller for Visual Tracking of Constrained Robot Manipulators

R. García-Rodríguez, E. Dean-León, V. Parra-Vega, and F. Ruíz-Sánchez

Abstract— **Diverse image-based tracking schemes of robot moving in free motion have been proposed, and experimentally validated, whose position and velocity image tracking errors converge to zero. However, visual servoing for constrained motion robot tasks has not been addressed so as to provide control schemes that guarantee simultaneous tracking of position, velocity and contact force trajectories for dynamic robot models. The main difficulty may steam from the fact that camera information cannot be used to drive force trajectories.Recognizing this fact, in this paper a unique error manifold that includes position-velocity errors and force errors in orthogonal complements is proposed under the framework of passivity, to yield a synergetic scheme that fuses camera, encoder and force sensor signals. This seemingly fusion of all tracking errors into a unique error variable allows to propose a new control system which guarantees local exponential tracking of all error trajectories. A neural network, driven by an orthogonalized second order sliding mode surface is derived to compensate approximately for nonlinear robot dynamics. Residual errors that arises because of the finite size o the neural network are finally eliminated via two sliding modes. Simulations results are presented and discussed.**

Index Terms— **Visual Servoing, Neural Network Control, Force Control, Multifusion Sensor, Robot Manipulator**

I. INTRODUCTION

Model-based hybrid vision/force control approaches have been reported [1], [6], [10], [2], [5], [14], but none of them shows robustness to uncertainties, robot parameters nor camera parameters. In a different path, [15] presents an interesting scheme of hybrid vision force control in an uncalibrated environment, with a very complex control law. With respect to force control, [11] proposed a judicious design of the extended error based on the orthogonalization principle which establishes the orthogonal decomposition of the error space to include all error signals into a unique error variable, however these schemes have not been extended, or combined, beyond constrained robots with state feedback.

Recently, and based on our previous results on adaptive force control with unknown model [12], and dynamic visual servoing [13], we proposed an adaptive hybrid visual servoing [3], which guarantees simultaneous tracking of position, velocity and force trajectories. However, all these schemes depend on the exact knowledge of the model, which is difficult to model in relevant practical applications.

A natural choice to get ride of the regressor is a neural network-based controller, because the ability of the neural network to approximate the regressor. However, usually *"small size"* neural network does not approximate exactly the input-output map of nonlinear systems, and furthermore, it may require a very dense network to deliver bounded approximate error. Therefore, we must proceed with caution since the holonomic constraint of a DAE [1] system, such a constrained robot, must be fulfilled for all time, and the approximation error of the neural network may provoke inconsistency of the DAE system. That is, synthesizing an image-based neural network for constrained robots is not straightforward.

A. The problem

The problem we are interested in may be resumed as follows: *Design a control system that guarantees fast image-based tracking of constrained robots, subject to unknown regressor.* This problem is still an open in the literature.

B. Contribution

A neural network-based control for simultaneous tracking of visual position and contact force trajectories of unknown constrained robots is proposed. The key is the orthogonalization of the extended error, which induces chattering-free second order sliding modes in each orthogonal complements. These orthogonal sliding modes tune the neural network so as to provide fast and well posed approximate compensation of nonlinear robot dynamics. The residual error that arises from this bounded compensation is yet eliminated with the sliding modes in each orthogonal subspace. Finally, local exponential tracking of image-based position error and contact force error arises.

The *low dimensional neural network*requires only one layer with one neuron per degree of freedom, and four weights per neuron. The underlying reason that allows to obtain this result is the derivation a new image-based orthogonalized principle. Thus, similar results to the case of nonvisual-based orthogonalized principle are obtained. This nontrivial extension of force control merges our previous results on force control, second order sliding mode, and dynamic visual servoing. Simulations allows to visualize the expected closed loop performance predicted by the theory.

[1]Dynamical Algebraic System (DAE) robots carry out two motion task, where the end-effector is in contact to a rigid unconformable surface, exerting force on it and in its orthogonal direction, the end effector move. constrained motion task are defined as the exertion of a desired profile of force in the constrained force degrees of freedom (f-DOF), while simultaneously moving along the unconstrained position degrees of freedom (p-DOF). The dynamics that arises in such motion are defined by the set of n($=f+p$) DOF coupled to an algebraic constrain. Together renders a DAE of order 2

Mechatronics Division, CINVESTAV, AP 14-740, México, D.F., México
(rgarciar,edean,vparra,fruiz)@mail.cinvestav.mx

II. NONLINEAR ROBOT DYNAMICS

A. Visual Kinematics

Direct and differential kinematics of a serial $n-$link rigid robot manipulator are given, respectively, by

$$x_b = f(q) \qquad \dot{x}_b = J(q)\dot{q} \tag{1}$$

where $x_b \in \Re^n$ represents the position of robot end effector in operational workspace, in our case the cartesian space, $q \in \Re^n$ is the vector of generalized joint displacements, finally $f(\cdot) : \Re^n \to \Re^n$, and $J(q)$ as the analytical jacobian.

In this case, consider the camera model, using thin lens without aberration, [8] presented the widely accepted fixed (static) camera configuration, whose basic mathematical description of this system consists of a composition of four transformations defined as follows

- Joint to Cartesian transformation
- Cartesian to Camera transformation
- Camera to CCD transformation
- CCD to Image transformation

Then we have the following forward visual kinematics. Note that the visual position $x_s \in \Re^2$ of robot end effector in image space (screen) is given by

$$\begin{aligned} x_s &= \alpha_0 \frac{\lambda_f}{\lambda_f - z} \begin{bmatrix} -1 & 0 \\ 0 & 1 \end{bmatrix} R_0 x_b + \beta & (2) \\ &= \alpha R x_b + \beta & (3) \end{aligned}$$

where α_0 is the scale factor [2], $R_0 \in R^{2\times 2}$ stands for the 2x2 upper square matrix of $R_\theta \in SO(3)$, that is

$$R_0 = \begin{bmatrix} -\cos(\theta) & \sin(\theta) \\ \sin(\theta) & \cos(\theta) \end{bmatrix} \tag{4}$$

and

$$R = \begin{bmatrix} \cos(\theta) & -\sin(\theta) \\ \sin(\theta) & \cos(\theta) \end{bmatrix} \quad \alpha = \alpha_0 \frac{\lambda_f}{\lambda_f - z} \tag{5}$$

$$\beta = \alpha_0 \frac{\lambda_f}{\lambda_f - z} \begin{bmatrix} {}^v O_{b1} \\ {}^v O_{b2} \end{bmatrix} + \begin{bmatrix} u_c \\ v_c \end{bmatrix} \tag{6}$$

where λ_f is the focal distance along optical axis, z stands for the depth of field, u_c, v_c define the translation of camera center to image center, and ${}^v O_{b1}, -{}^v O_{b2}$ define the distance between optical axe and the robot base $\vec{Z}$. In this way, the differential camera model is then

$$\dot{x}_s = \alpha R \dot{x}_b \tag{7}$$

Notice that the constant transformation αR maps statically *robot* cartesian velocities into *visual* cartesian velocities, and the *visual flow* $\dot{x}_s$ does not contain any independent input. Now, using equation (1)$\sim$(7), we have a equation that relates image velocities with joint velocities as follows

$$\dot{x}_s = \alpha R J(q)\dot{q} \tag{8}$$

[2]Without lose of generality, α_0 can be considered as a scalar matrix 2×2.

where $\dot{x}_s \in \Re^2$ determines the visual robot end effector velocity and notice that $\alpha R J(q)$ maps joint velocities to *visual* cartesian velocities. To obtain the inverse differential visual kinematics, solve equation (8) for $\dot{q}$

$$\dot{q} = J_{Rinv} \dot{x}_s \tag{9}$$

where, the simplification $J_{Rinv} = J(q)^{-1} R^{-1} \alpha^{-1} = J(q)^{-1} R_\alpha^{-1}$, has been used. With $J_{Rinv} \in \Re^{n\times n}$ whose entries are function of robot and camera parameters.

B. Constrained Robot Dynamics

Using the *Constrained Lagrangian* ($L_c = K - P + \varphi(q)^T \lambda$), the constrained robot dynamics arises as a set of differential algebraic equations as follows

$$\begin{aligned} H(q)\ddot{q} + (B_0 + C(q,\dot{q}))\dot{q} + g(q) &= \tau + J_\varphi^T(q)\lambda & (10) \\ \varphi(x,w) &= 0 & (11) \end{aligned}$$

where $H(q) \in R^{n\times n}$ is the symmetric positive definite manipulator inertia matrix, $B_0 \in \Re^{nxn}$ stands for a diagonal positive definite matrix composed of damping friction for each joint, $C(q,\dot{q})\dot{q} \in R^n$ stands for the vector of centripetal and coriolis torques, $g(q) \in R^n$ is the vector of gravitational torques, $\lambda \in R^n$ is a vector of Lagrange multipliers or contact forces, and finally $\varphi(x,w)$ is the kinematic restriction, as a rigid surface and frictionless, where, $\varphi = (x,w) : \Re^n \to \Re$ is a given scalar function, with $x = (x_1, x_2, x_3)^T$ denoting a position of a fixed coordinated system and $w = (w_1, w_2, w_3)^T$ its associated Euler angles.

C. Parametrization of Robot Dynamics

The robot dynamic model complies with the property known as *dynamic linear parametrization*, this is, the robot dynamic is lineally parameterizable in terms of a known regressor $Y_b = Y_b(q,\dot{q},\ddot{q}) \in \Re^{n\times p_1}$ and an unknown constant vector $\theta_b \in \Re^{p_1}$ of robot parameters, as follows

$$H(q)\ddot{q}_r + (B_0 + C(q,\dot{q}))\dot{q}_r + g(q) = Y_b \theta_b \tag{12}$$

Adding and subtracting the lineal model parametrization to equation (10), we have the open loop error equation as

$$H(q)\dot{S}_q = \tau + J_\varphi^T(q)\lambda - Y_b\theta_b - (B_0 + C(q,\dot{q}))S_q \tag{13}$$

with S defined by

$$S_q = \dot{q} - \dot{q}_r \tag{14}$$

which is called as the joint error surface, and $\dot{q}_r$ is a nominal reference of joint velocities, and is, so far, not yet defined. Notice that (14) can be written, using (9), by $S_q = J_{Rinv}\dot{x}_s - \dot{q}_r$ thus, we are tempted to design $\dot{q}_r = f(J_{Rinv}\dot{x}_{sd}, \lambda_d)$, for $\dot{x}_{sd}$ the desired reference of image velocity trajectory, and λ_d the desired contact force. To this end, let first design a *Visual Orthogonalization Principle* to obtain a unique error variable composed of both visual position and force errors.

III. OPEN LOOP ERROR EQUATION

A. Visual Orthogonalization Principle.

Since $\varphi(q) = 0 \forall t$, then its time derivative yields

$$\frac{d}{dt}\varphi(q) = \frac{\partial \varphi(q)}{\partial q}\frac{dq}{dt} \equiv J_\varphi(q)\dot{q} \doteq 0 \quad (15)$$

This means that $J_\varphi(q)$ is orthogonal to $\dot{q}$. That is, $\dot{q}$ belongs to the orthogonal projection matrix Q of $J_\varphi(q)$ [11]

$$Q = I - \frac{J_\varphi^T}{\left\|J_\varphi(x)\right\|^2} J_\varphi \quad (16)$$

Clearly, Q spans the tangent plane at the contact point, thus

$$Q\dot{q} = \dot{q} \quad (17)$$

and

$$QJ_\varphi^T = 0$$

Therefore, J_φ and Q are orthogonal complements since R^n is generated by the direct sum of two orthogonal sub-spaces, since $rank(im(Q)) = m \equiv n-r$ and $rank\left(im\left(J_\varphi\right)\right) = r$, such as $m+r=n$. In other words, These facts are fundamental to solve the problem.

B. Nominal Orthogonalized References

Notice that the *visual orthogonalization principle is established in visual space at the velocity level*, we need to introduce an orthogonalized reference signal $\dot{q}_r = \dot{q}_s + \dot{q}_f$ at the velocity level, where $\dot{q}_s^T \dot{q}_f = 0$. Thus consider

$$\dot{q}_r = QJ_{Rinv}\dot{x}_r + \beta J_\varphi^T \dot{q}_{rf} \quad (18)$$

where $\beta > 0$ and $\dot{x}_r$ and $\dot{q}_{rf}$ stand for the visual position nominal reference and force nominal reference, respectively.

1) Visual position nominal reference: Using definition of (9),consider

$$\dot{x}_r = \dot{x}_{sd} - \alpha\Delta x_s + S_{sd} - \gamma_s \int_{t_0}^{t} sign(S_{s\delta}) \quad (19)$$

where, $\alpha > 0, \gamma_s > 0$ are positive definite feedback gains, $\dot{x}_{sd}$ stands for desired visual trajectory velocity, $\Delta x_s = x_s - x_{sd}$ is the visual position error, and

$$S_{s\delta} = S_s - S_{sd}, \quad S_s = \Delta\dot{x}_s + \alpha\Delta x_s, \quad S_{sd} = S_s(t_0)e^{-\kappa_s t}$$

where $\Delta\dot{x}_s = \dot{x}_s - \dot{x}_{sd}$, defines visual velocity error, κ_s is a positive constant and the function $sign(y)$ stands for sign function of vector y, and finally defining $\int_{t_0}^{t} sign(Y) \equiv \int_{t_0}^{t} sign(Y(\zeta))d\zeta$.

2) Force nominal reference: Let the nominal force reference be

$$\dot{q}_{rf} = \Delta F - S_{dF} + \gamma_F \int_{t_0}^{t} sign(S_{F\delta}) \quad (20)$$

for $\gamma_F > 0$ is a positive definite gain and

$$S_{F\delta} = S_F - S_{Fd}, \quad S_F = \Delta F, \quad S_{Fd} = S_F(t_0)e^{-\kappa_F t}$$

with $\kappa_F > 0, \Delta F = \int_{t_0}^{t} \Delta\lambda$ and $\Delta\lambda = \lambda - \lambda_d$.

C. Joint Error Surface

Substituting (18), (19), (20) into (14), by using (9), we obtain the following visual orthogonalized joint error surface

$$\begin{aligned} S_q &= \dot{q} - \dot{q}_r \\ &= QJ_{Rinv}(\dot{x}_s - \dot{x}_r) + \beta J_\varphi^T \dot{q}_{rf} \\ &= QJ_{Rinv}S_{vs} - \beta J_\varphi^T S_{vf} \end{aligned}$$

where

$$S_{vs} = S_{s\delta} + \gamma_s \int sign(S_{s\delta})$$

$$S_{vf} = S_{F\delta} + \gamma_F \int sign(S_{F\delta})$$

D. Open Loop Error Dynamics

Since $\ddot{q}_r$ is discontinuous, and neural network can approximate only continuous mappings, then we need to rewrite it follows

$$\begin{aligned} \ddot{q}_r &= \dot{Q}J_{Rinv}\dot{x}_r + Q\dot{J}_{Rinv}\dot{x}_r + QJ_{Rinv}\ddot{x}_r \\ &\quad + \beta\dot{J}_\varphi^T\dot{q}_{rf} + \beta J_\varphi^T\ddot{q}_{rf} \quad (21) \\ &= \ddot{q}_{cont} + \ddot{q}_{disc} \quad (22) \end{aligned}$$

where

$$\begin{aligned} \ddot{q}_{cont} &= \dot{Q}J_{Rinv}\dot{x}_r + Q\dot{J}_{Rinv}\dot{x}_r + QJ_{Rinv} * \\ &\quad (\ddot{x}_{sd} - \alpha\Delta\dot{x}_s + \dot{S}_{sd} - \gamma_s \tanh(\lambda_p S_{s\delta})) + \\ &\quad \beta\dot{J}_\varphi^T\dot{q}_{rf} + \beta J_\varphi^T(\Delta F - \dot{S}_{dF} + \gamma_F \tanh(\lambda_f S_{F\delta})) \\ \ddot{q}_{disc} &= QJ_{Rinv}Z_p - \beta J_\varphi^T Z_f \quad (23) \end{aligned}$$

with $Z_p = \tanh(\lambda_p S_{s\delta}) - sgn(S_{s\delta}), Z_f = \tanh(\lambda_f S_{F\delta}) - sgn(S_{F\delta})$ for $\tanh(*)$ as the continuous hyperbolic tangent function of $(*)$ and $\lambda_p, \lambda_f \in \Re^{nxn} > 0$. The continuous function $\tanh(.)$ is used as approximation of discontinuous function $sgn(.)$, such that $\tanh(0) = 0$ and $\tanh(\lambda_p S_{qp}) \to sgn(S_{qp})$, $\tanh(\lambda_f S_{qf}) \to sgn(S_{qf})$ when $\lambda \to \infty$. Notice that Zp, Zf have the following properties: $Z \geq -1$, $Z \leq +1$, $Z_{S_q \to 0^-} = -1$, $Z_{S_q \to 0^+} = +1$ and $Z_{S_q \to \pm\infty} = 0$. Finally, note that $Y_{cont} = Y_b(q, \dot{q}, \dot{q}_r, \ddot{q}_r)$ is continuous due to $(\dot{q}_r, \ddot{q}_{cont}) \in \mathscr{C}^1$and Z_p, Z_f are discontinuous, but bounded. Substituting (18) into (12) give rise to

$$H(q)\ddot{q}_r + (B_0 + C(q,\dot{q}))\dot{q}_r + G(q) = Y_{cont}\Theta + \tau_d \quad (24)$$

where $\tau_d = H(q)\ddot{q}_{disc}$ is considered as an endogenous bounded disturbance, which cannot be compensated by the neural network since it is discontinuous. Then, (24) into (10) the open loop error equation finally arises

$$H(q)\dot{S}_q + (B_0 + C(q,\dot{q}))S_q = \tau - Y_{cont}\Theta + J_\varphi^T(q)\lambda + \tau_d \quad (25)$$

At this stage, before to design τ, it remain to discuss the design of the neural network scheme as an associator to approximately compensate for $Y_{cont}\Theta$.

IV. NEURAL NETWORK APPROXIMATOR

Let $\mathbf{K}$ be a closed bounded subset of $\Re^n$ and a real vector valued functions $f(*)$ be defined on $\mathbf{K}$ as $f:\mathbf{K}\subset\Re^n\rightarrow R$. We would like to approximate function $f(*)$ by using tree structure [7] in which many neurons on one layer feed a single neuron on the next layer, is a generic architecture for networks satisfying the Stone-Weierstrass theorem with linear functions for the input and output layers. The input-output relationship for this generic architecture is given as $Y=f(x)=\phi(\sum_{i=1}^{n}W^TX)$ where W, X y Y represent the weights, inputs to the unit and output from the unit, respectively. It's important to notice that the tree structure has one or more hidden layers followed by a linear output neuron by means of which its possible to create multilayer neural network with an arbitrary number of neurons in each hidden layer. In this work we use ϕ as a linear function i.e. function approximation is parameterized by static adaline neural network.

Based on the Stone-Weierstrass theorem [7] show that any smooth functions $f(x)\in C^m(\mathbf{S})$, where $\mathbf{S}$ is a compact set simply connected set of $\Re^n$, can be approximated by a sufficiently large dimensional neural network, given as

$$\hat{f}(x)=\phi(\mathbf{W}_1^TX)$$

where the bounded weight vector $\mathbf{W}$ is optimal (in a sense that $f(x)-\hat{f}(x)=0$) and X belong to a compact set $\mathbf{K}\subset\Re^{2n}$, that is $\mathbf{S}:=\{x:\|x\|\leq\mathbf{S}\}$. And, if the approximation is done with a low dimensional neural network, then a bounded functional reconstruction error $\varepsilon(x)$ appears

$$\hat{f}(x)=\phi(\mathbf{W}_2^TX)+\varepsilon(x)$$

where $\mathbf{W}_2^T$ is a subset of $\mathbf{W}_1^T$ and $\|\varepsilon(x)\|\leq\varepsilon_N$, con $\varepsilon_N>0$.

In this paper, the unknown nonlinear function $f(x)=Y_{cont}\Theta$, is approximated by static adaline neural network with output $\hat{f}(x,\mathbf{W}_{n2})=\mathbf{W}_{n2}^TX$ where $\mathbf{W}_{n2}^T\in\Re^{n2}$ is the matrix of adjustable weights and $n2$ denotes a low number of weights, with $n2\ll n1$. The main reason for selecting this type of neural network is that this network provides very easy way to approximate $f(x)$ without worrying about its accuracy. Besides this, the size $n2$ of the network can be obtained roughly by checking carefully the dynamics of a general n-link rigid arm. Now, let consider the approximation of $f(x)$ as follows[3]

$$\hat{f}(x)=Y_{cont}\hat{\Theta}=\hat{\mathbf{W}}^TX+\varepsilon(x) \tag{26}$$

where $Y_{cont}\Theta\in\Re^{nxp}$, $\Theta\in\Re^{px1}$ stand for the function to be approximated

$$X=(q,\dot{q},\dot{q}_r,\ddot{q}_{cont})\in R^{2n}$$

In this way, using low dimensional neural network, the estimation of $f(x)$ is $\hat{f}(x)$, where $\hat{f}(x)$ stands for the online estimation of $Y_{cont}\Theta$. Now we are ready to design the neural network adaptive controller.

[3]Without of generality, in the rest of the paper we refer $\mathbf{W}_{n2}$ as $\mathbf{W}$, omitting its subindex

Remark 1. The difference of our approach with respect to [4], [9] and many others, is that we propose a low dimensional neural network, based on linear associator and still we are able to prove convergence, in contrast to those references that guarantee only bounded tracking.

Remark 2. Notice that the dimension of the neural network is very low, it is composed of decentralized neurons, that is the neurons of the i degree of freedom depend only on data of the state i and variables related only to i. For instance, for a two degrees of freedom system, $n_2=2$, thus $2n=4$, so we have two neurons with a four weights each one.

Our controller presented in the next section, will compensate $Y_{cont}\Theta$ with a low dimensional neural network, while the approximation error of the neural network and Z_p, Z_f in τ_d, will be compensated with an orthogonalized second order sliding mode inner loop. Notice that endogenous bounded terms Z_p, Z_f and τ_d are casted as disturbances.

V. CONTROL DESIGN

Substituting (26) in (25) becomes

$$H(q)\dot{S}_q+(B_0+C(q,\dot{q}))S_q=\tau-\mathbf{W}^T\mathbf{X}+J_\varphi^T(q)\lambda-\bar{\tau}_d \tag{27}$$

where $\bar{\tau}_d=\varepsilon(x)-\tau_d$. Now consider the following state feedback continuous control law

$$\begin{aligned}\tau &= -K_dS_q+\hat{\mathbf{W}}^TX+J_\varphi^T(q)[-\lambda_d+\eta\Delta F]+\\ &\quad \gamma_FJ_\varphi^T(q)[sgn(S_{F\delta})+\eta\int_{t_0}^{t}sgn(S_{F\delta})] \qquad (28)\\ \dot{\hat{\mathbf{W}}} &= -\Gamma X^TS_q \qquad (29)\end{aligned}$$

with $K_d=K_+^T\in\Re^{nxn}$, $\Gamma=\Gamma^T\in\Re^{pxp}$ diagonals and definite positives, λ_d is desired contact force. Substituting (28)-(29) into (27) the closed loop equation becomes

$$\begin{aligned}H(q)\dot{S}_q &= -[K+C(q,\dot{q})]S_q-\Delta\mathbf{W}X+\\ &\quad J_\varphi^T(q)[\dot{S}_{vf}+\eta S_{vf}]+\bar{\tau}_d \qquad (30)\\ \Delta\dot{\mathbf{W}} &= \Gamma X^TS_q \qquad (31)\end{aligned}$$

where $\bar{\tau}=\bar{\tau}_d-\gamma_2J_\varphi^T(q)Z$, $Z=tanh(\mu S_{F\delta})-sgn(S_{F\delta})$, $K=K_d+B_0$, $\Delta\mathbf{W}=W-\hat{W}$, $\hat{\mathbf{W}}\in\Re^{nxp}$ stands for the neural network weights, $X\in\Re^{px1}$ stands for the input to the network, and $\Gamma=\Gamma^T\in\Re_+^{pxp}$. Now, we can state the stability properties in the next theorem.

Theorem. (Second Order Sliding Mode Constrained Visual Neural Network) Consider a constrained robot manipulator (10)-(11) under the continuous model free second order sliding mode scheme (28)-(29), and assume that the feedback gains K_d,η,β are large enough, and errors on initial condition are small enough. Then the closed loop system yields local exponential convergence of visual and force tracking errors. Furthermore, a second order sliding mode is enforced for all time with a low dimensional neural network, and with smooth control effort.

Proof. See Appendix section.

A. Discussion

Remark 3. We have proved that $J(q)(t_0)$ is not singular for all time, because $J_{Rinv} = J^{-1}(q) R_{\alpha}^{-1}(\theta)$ at a given initial conditions, and because desired trajectories belong to robot workspace Ω, and trajectories converge with an exponential envelope.

Remark 4: Adaptive Neural Network. It is fundamental the contribution of the neural network for this scheme to work, since it compensates robot dynamics in orthogonal subspaces, it is in fact a DAE approximator with very low computational load since it is required only few nodes to bound the approximation error.

Remark 5: Two Orthogonal Sliding Mode Regimes. Worth to mention that two sliding mode regimes arises, each one in the complementary spaces spanned by Q and J_{φ}^{T}, and the establishment are each other independent.

Remark 6: Continuous Control. Clearly the controller does not involves discontinuous signals, which is very relevant for real time implementation purposes.

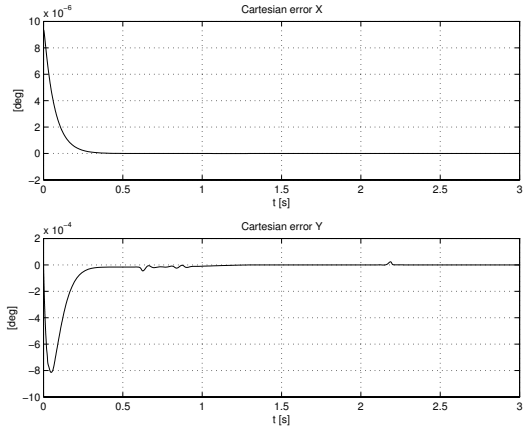

Fig. 1. Cartesian tracking error,mapped from image-based position error.

VI. SIMULATIONS

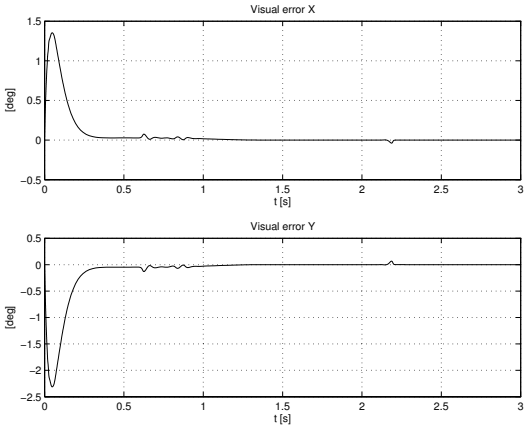

Fig. 2. Visual errors with exponential convergence.

Digital simulations on the 2-DOF nonlinear model of a rigid arm are presented. The stiff numerical solver of Matlab 5.3 was implemented, under $1s$ sampling simulation time. The end-effector of the rigid robot arm is in contact with a rigid wall, simulating a polishing task, wherein a given sinusoidal profile of force is exerted in the normal direction, while moving along the wall. The robot parameters are take from a real 2DOF planar robot, available in the laboratory, together with real parameters of a SONY DFWVL500 CCD camera, see Tables (I) and (II). Desired trajectories are $x_s = \alpha R[xcd; ycd] + \beta, xcd = 0.5; ycd = 0.5 + r * \sin(w * t)$; $r = 0.1$, $w = 0.5$. Contact surface is a plane parallel to plane YZ and over $x = 0.5$ and $\lambda_d = 20 + 8sin(5t)N$ Feedback gains $\kappa_f = 20, \gamma_f = 6.1, \eta = 0.029, \beta = 3.0, K_d = 60, \alpha = 25, \kappa_s = 20, \gamma_s = 3.12, \Gamma = 20$.

As expected, the end-effector tracks the desired cartesian trajectory without any knowledge of robot dynamics nor inverse kinematics. After a very short transient, due to numerical problems of the DAE solver, simultaneous force-position exponential tracking is established, (Fig. 3) with relatively smooth control effort i.e there is no over saturation (Fig. 4). In Fig. (2), shows the visual position error, where the systems converge to an error that can be considered as zero. (less than 0.1 pixel error) and Fig. (1), shows that cartesian errors shows exponential convergence.

TABLE I
ROBOT PARAMETERS.

Robot parameter	Value
Length link l_1, l_2	$0.4, 0.3\ m$
Center of gravity 1,2 l_{c1}, l_{c2}	$0.1776, 0.1008\ m$
Mass link m_1, m_2	$9.1, 2.5714\ kg$
Inertia link I_1, I_2	$0.284, 0.0212\ kgm^2$

TABLE II
CAMERA PARAMETERS.

Vision parameters	Value
Clock-wise rotation angle θ	$\frac{\pi}{2}\ rad$
Scale factor α_v	$77772\ pixeles/m$
Depth field of view z	$1.5\ m$
Camera offset ${}^{v}O_b$	$[-0.2 \quad -0.1]^T\ m$
Offset $\Sigma_I\ o_I$	$[0.0005 \quad 0.0003]^T\ m$
Focal length λ_f	$0.008\ m$

VII. CONCLUSIONS

A novel scheme for neural constrained image-based force-visual servoing for robot arms is proposed. It is shown the local exponential convergence in the position-velocity and force subspaces, even when neither robot parameters nor camera parameters are known, only the analytical jacobian is required. The main feature or our scheme is the ability to fuse image coordinates into an orthogonal

complement of joint velocities, and contact forces in the orthogonal complement of integral of contact forces. The neural network control loop compensates for DAE dynamics while an inner piecewise continuous sliding mode control loop adds the missing effort to induce sliding modes. No training for the neural network is required. A formal proof of stability is given, and simulation results show that high performance achieved.

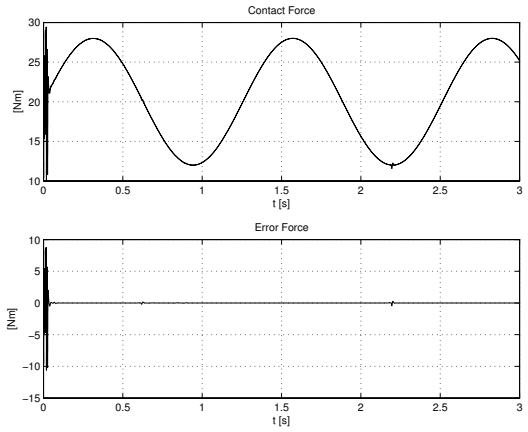

Fig. 3. Tracking of cartesian sinusoidal contact force and force error

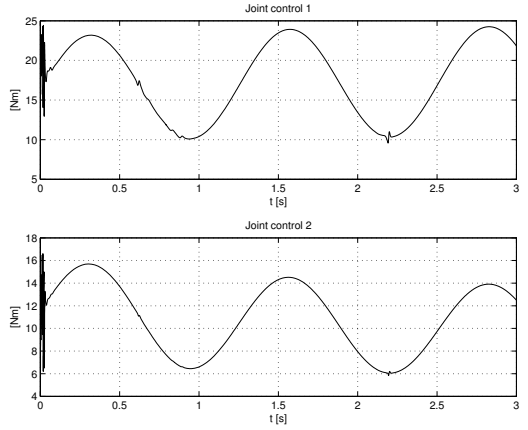

Fig. 4. Smooth control inputs for each joint.

APPENDIX

Proof of Theorem 1 A passivity analysis $\langle S, \tau* \rangle$ indicates that the following candidate Lyapunov function V qualifies as a Lyapunov function

$$V = \frac{1}{2}\{S_q^T H S_q + \beta S_{vf}^T S_{vf} + \Delta \mathbf{W}^T \Gamma^{-1} \Delta \mathbf{W}\}$$

where $\beta > 0$ is a scalar. The total derivative of Lyapunov along its solution (30) immediately leads to

$$\begin{aligned} \dot{V} &= -S_q^T K S_q - \beta \eta S_{vf}^T S_{vf} + S_r^T \bar{\tau}_d \\ &\leq -S_q^T K S_q - \beta \eta S_{vf}^T S_{vf} + \|S_r^T\| \|\delta\| \end{aligned} \tag{32}$$

where $K = K_d + B_0$, δ is a functional that bounds $\bar{\tau}$ and and its existence arises due to the boundedness of feedback gains, the smoothness of $\varphi(x)$ (such that assures upper bound for Q,J_φ, $J_{Rinv}(q)$, J(q)),$\gamma_2 J_\varphi^T Z$ and finally the boundedness of Z. In the same way we have used the skew symmetric property of $\dot{H} - 2C$. All this arguments establish the existence of the functional $\delta = f(S_{vs}, S_{vf}, H(q), C(q,\dot{q}), g(q), \varphi(x), X)$. Then K_d, β and η are large enough and the initial errors are small enough, we conclude the seminegative definiteness of (32) outside of hyperball $\varepsilon_0 = \{S_q | \dot{V} \leq 0\}$ centered at the origin, such as the following properties of the state of closed loop system arise $S_q \in \mathscr{L}_\infty \rightarrow \|S_q\| \leq \varepsilon_1$with $\varepsilon_1 > 0$. Then, $(S_{s\delta}, \int sign(S_{s\delta})) \in \mathscr{L}_\infty$ and since desired trajectories are C^2 and feedback gains are bounded, we have that $(\dot{q}_r, \ddot{q}_r) \in \mathscr{L}_\infty$, which implies that $Y_{cont} \in \mathscr{L}_\infty$. The right hand side of (30) shows that $\varepsilon_2 > 0$ exists such that $\|\dot{S}_q\| \leq \varepsilon_2$ This result stands for local stability of S_q provided that the state is near the desired trajectories for any initial condition. Now we prove that the sliding mode arises.

Part II. Sliding modes (visual tracking and force). Since $S_q \in \mathscr{L}_2$, and J_{Rinv} and Q are bounded (is easily to prove that if $J(q)$ is bounded then J_{Rinv} is bounded), then $QJ_{Rinv}S_{vs}$ is bounded and, due to $\varphi(q)$ is smooth and lies in the reachable robot space and $S_{vF} \rightarrow 0$, then $\beta J_\varphi^T S_{vF} \rightarrow 0$. Now, taking into account that $\dot{S}_q$ is bounded, then $\frac{d}{dt} J_{Rinv} Q S_{vs}$ and $\frac{d}{dt} \beta J_\varphi^T S_{vf}$ are bounded (this is possible because J_φ^T is bounded and so $\dot{Q}$ is). All this chain of conclusions proves that there exists constants $\varepsilon_3 > 0$ and $\varepsilon_4 > 0$ such that $|\dot{S}_{vs}| < \varepsilon_3, |\dot{S}_{vf}| < \varepsilon_4$Now, we have to prove that for a proper γ_s and γ_F, we can conclude that trajectories of visual position and force converges to zero. This is possible through sliding modes for the subspace of visual position Q and the subspace of force $J_\varphi^T(q)$. Considering that operator QJ_{Rinv} spans the vector $\hat{S}_q$ in its image $im\{QJ_{Rinv}(S_{vs})\} \equiv S_{vs}^{im}$ and the operator βJ_φ^T spans the same vector in its image $im\{\beta J_\varphi^T(S_{vf})\} \equiv S_{vf}^{im}$, this implies that

$$S_q = QJ_{Rinv}S_{vs} - \beta J_\varphi^T S_{vf} \Rightarrow = S_{vs}^{im} - S_{vf}^{im} \tag{33}$$

where S_{vs}^{im} and S_{vf}^{im} belongs to a orthogonal complements, that means $\langle S_{vs}^{im}, S_{vF}^{im} \rangle = 0$. We are able to analyze the S_{vs}^{im} dynamics, independently of S_{vf}^{im}, since S_{vf}^{im} belongs to the kernel of Q. This is verified if we multiply (33) for Q^T,

$$Q^T S_q = Q^T QJ_{Rinv}S_{vs} - \underbrace{\beta Q^T J_\varphi^T \{S_{vf}\}}_{\text{equal } 0} \Rightarrow S_{vs}^{im} \tag{34}$$

since Q is idempotent $(Q^T Q = Q)$. It is important notice that if $Ax = Ay$ for any square matrix A and any couple of vectors x, y, then $x \equiv y$. Thus, the equation (34) means that for the subspace Q, the equality $S_q = QJ_{Rinv}S_{vs}$ is valid within span of Q.

Part II.a: Exponential convergence of visual tracking errors. According to $Q^T \hat{S}_q = QJ_{Rinv}S_{vs}$ then $S_q \equiv J_{Rinv}S_{vs}$ in the subspace image of Q, however notice that Q is not

full rank, then this equality is valid locally, not globally. In this local neighborhood, if we multiply the equality $S_q = QJ_{Rinv}S_{vs}$ by $R_\alpha(\theta)J(q)$ ($J_{Rinv} = J^{-1}(q)R_\alpha^{-1}(\theta)$), we have

$$R_\alpha(\theta)J(q)S_q = S_{vs} \equiv S_{s\delta} + \gamma_s \int sign(S_{s\delta}) \quad (35)$$

Taking the time derivative of the above equation, and multiply it by $S_{s\delta}^T$ produces

$$\begin{aligned} S_{s\delta}^T \dot{S}_{s\delta} &= -\gamma_s S_{s\delta}^T sign(S_{s\delta}) + S_{s\delta}^T \frac{d}{dt}[R_\alpha(\theta)J(q)S_q] \\ &\leq -\gamma_s |S_{s\delta}| + \varepsilon_5 |S_{s\delta}| \\ &\leq -\mu_s |S_{s\delta}| \end{aligned} \quad (36)$$

where $\varepsilon_5 = \frac{d}{dt}[R_\alpha(\theta)J(q)S_q]$, and $\mu_s = \gamma_s - \varepsilon_5$. Thus, we obtain the sliding condition if

$$\gamma_s > \varepsilon_5$$

such as, $\mu_s > 0$ of (36) guarantee the sliding mode at $S_{s\delta} = 0$ in a time $t_s = \frac{|S_{s\delta}(t_0)|}{\mu_s}$. However, notice that for any initial condition $S_{s\delta}(t_0) = 0$, then $t_s = 0$, which implies that the sliding mode at $S_{s\delta}(t) = 0$ is guaranteed for all time. Then, we have

$$S_s = S_{sd} \forall t \rightarrow \Delta\dot{x}_s = -\alpha\Delta x_s + S_s(t_0)e^{-\kappa_s t}$$

this implies that the visual tracking errors locally tends to zero exponentially fast, this is

$$x_s \rightarrow x_{sd}, \quad \dot{x}_s \rightarrow \dot{x}_{sd}$$

implying that the robot end-effector converges to the desired image x_{sd}, with given velocity $\dot{x}_{sd}$.

Part II.b: Exponential convergence of force tracking errors. If we multiply S_q for J_φ we have:

$$J_\varphi S_q = \underbrace{J_\varphi Q J_{Rinv} S_{vs}}_{\text{equal to } 0} - \beta J_\varphi J_\varphi^T \{S_{vf}\} \Rightarrow S_{vf}^{im} \quad (37)$$

Now, if we multiply 37 for $\left(J_\varphi J_\varphi^T(q)\right)^{-1}$, we obtain

$$J_\varphi^\#(q)S_q = S_{vF} \equiv S_{F\delta} + \gamma_F \int sign(S_{F\delta})$$

where $J_\varphi^\#(q) = \left(J_\varphi J_\varphi^T(q)\right)^{-1} J_\varphi$. Derivating the above equation and multiply for $S_{F\delta}^T$ lies

$$\begin{aligned} S_{F\delta}^T \dot{S}_{F\delta} &= -\gamma_F S_{F\delta}^T sign(S_{F\delta}^T) + S_{F\delta}^T \frac{d}{dt}\left(J_\varphi^\#(q)S_q\right) \\ &\leq -\gamma_F |S_{F\delta}| + |S_{F\delta}| \frac{d}{dt}\left(J_\varphi^\#(q)S_q\right) \\ &\leq -\gamma_F |S_{F\delta}| + |S_{F\delta}| \varepsilon_6 \\ &\leq -\mu_F |S_{F\delta}| \end{aligned}$$

where $\varepsilon_6 = \frac{d}{dt}\left[\left(J_\varphi J_\varphi^T(q)\right)^{-1} J_\varphi S_q\right]$. If $\gamma_F > \varepsilon_6$, then a sliding mode at $S_{F\delta}(t) = 0$ is induced in a time $t_f \leq \frac{|S_{F\delta}(t_0)|}{\mu_F}$, but $S_{F\delta}(t_0) = 0$, and that means $\Delta F = \Delta F(t_0)e^{-\kappa_F t}$. Moreover, in [11] it is showed that the convergence of force tracking errors arises, thus $\lambda \rightarrow \lambda_d$ exponentially fast. ■

REFERENCES

[1] A. Namiki, Y. Nakabo, I. I. M. I., High speed grasping using visual and force feedback. *Proceedings of the 1999 IEEE International Conference on Robotics and Automation*, Detroit, MI, pp 3195–3200.

[2] B. Nelson, Force and vision resolvability for assimilating disparate sensory feedback, *IEEE Trans. on Robot. and Autom.*, Vol.12 No. 5 pp 714–731.

[3] E.C. Dean-Leon, V. Parra-Vega, and A.Espinosa-Romero, Image-based Adaptive Position-Force Control for Robot Manipulators under Jacobian Uncertainty, *Int. Symposium on Robotics and Automation*, Queretaro, Mexico, August 25-28, 2004.

[4] F. L. Lewis, A. Yessildirek, y K. Liu, Multilayer Neural Net Robot Controller with Guaranteed Tracking Performance. *IEEE Trans. Neural Networks*, Vol. 6 No. 3 pp. 703-715.

[5] J. Baeten, W. Verdonck, H. B. J. D. S., Combining force control and visual servoing for planar contour following. *Machine Intelligence and Robotic Control*, Vol. 2 No.2 pp 69–75.

[6] N. Papanikolopoulus, P. Khosla, T. K., Visual tracking of a moving target by a camera mounted on a robot: A combination of control and vision, IEEE J. on Robot. and Autom., Vol. 9 pp 14–35.

[7] N. E. Cotter. The Stone-Weierstrass Theorem and Its Application to Neural Network. *IEEE Trans. on Neural Networks*, Vol. 1 No. 4, 1990 pp. 290-295.

[8] S. Hutchinson, G. Hager, P. C., A tutorial on visual servo control, Trans. on Robotics and Automation. Vol.12 No.5 pp.651-670

[9] S. S. Ge y C. C. Hang. Estructural Network Modeling and Control of Rigid Body Robots. *IEEE Trans. on Robotics and Automation*, Vol. 14 No. 5, 1998, pp. 823-827.

[10] T. Ishikawa, S. Sakane, T. S. H. T., Estimation of contact position between a grasped object and the environment based on sensor fusion of vision and force, *IEEE/SICE/RSJ Int. Conf. Multi-sensor Fusion and Integration for Intelligent Systems* Vol. 11 1996, pp 116–123.

[11] V. Parra-Vega and S. Arimoto, A Passivity-based Adaptive Sliding Mode Position-Force Control for Robot Manipulators,*International Journal of Adaptive Control and Signal Processing*, Vol. 10 1996, pp. 365-377.

[12] V. Parra-Vega, A. Castillo-Tapia, L. G. Garcia-Valdovinos, Decentralized model-free continuous control for robot manipulators: tracking in finite time ,*Proceedings of the Third International Workshop on Robot Motion and Control RoMoCo '02., 2002*., 9-11 Nov. 2002, pp 159–164

[13] V. Parra-Vega, J.D. Fierro-Rojas, Sliding PID uncalibrated visual servoing for finite-time tracking of planar robots. *IEEE International Conference on Robotics and Automation, 2003. Proceedings. ICRA '03*. Vol. 3, 14-19 Sept. 2003 pp 3042 - 3047.

[14] S. Jorg, J. Langwald, J. S. G. H. Chen, Flexible robot assambly using a multi-sensory approach. *Procc. of the 2000 IEEE Int. Conf. Robot. and Autom., San Francisco, CA*, pages 3687–3694.

[15] Xiao, D. (2000), Sensor-hybrid Position/Force control of a robot manipulator in an un calibrated enviroment. *IEEE Trans. Control Systm Technology*, Vol. 8 No. 4 pp 635–645.